Joule

CellPress

Article

Designing Artificial Solid-Electrolyte Interphases for Single-Ion and High-Efficiency Transport in Batteries

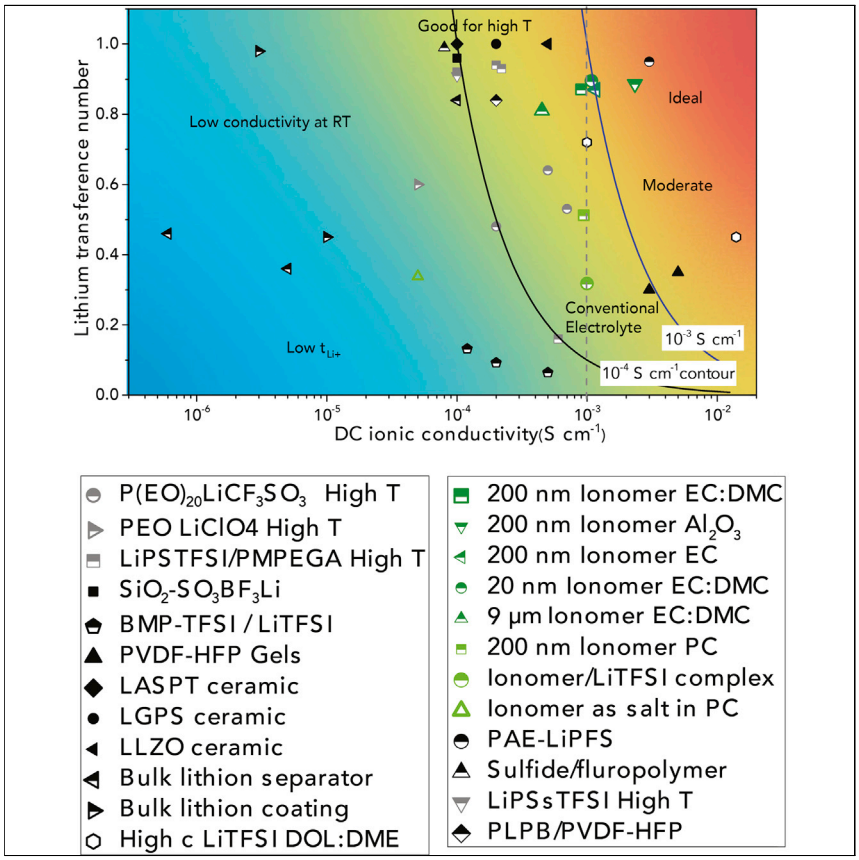

This article reports that high lithium transference number and high room temperature ionic conductivity can be simultaneously achieved in electrolytes by tethering nanometer-thick coatings of a single-ion conductor to an Li electrode. The protected electrode can be cycled stably at low and high currents.

Zhengyuan Tu, Snehashis Choudhury, Michael J. Zachman, Shuya Wei, Kaihang Zhang, Lena F. Kourkoutis, Lynden A. Archer

laa25@cornell.edu

HIGHLIGHTS

Ultrathin ionomer coatings on lithium-metal electrode enable stable electrodeposition

Nanometer-thick single-ion conductor coatings on electrodes eliminate ion polarization

Visualization studies show that ionomer coatings on Li prevent dendrite formation

Tu et al., Joule 1, 394–406
October 11, 2017
http://dx.doi.org/10.1016/j.joule.2017.06.002

Joule

CellPress

Article

Designing Artificial Solid-Electrolyte Interphases for Single-Ion and High-Efficiency Transport in Batteries

Zhengyuan Tu,[1,5] Snehashis Choudhury,[2,5] Michael J. Zachman,[3] Shuya Wei,[2] Kaihang Zhang,[2] Lena F. Kourkoutis,[3,4] and Lynden A. Archer[1,2,6,*]

SUMMARY

Substrates able to rectify transport of ions based on charge and/or size are ubiquitous in biological systems. Electrolytes and interphases that selectively transport electrochemically active ions are likewise of broad interest in all electrical energy storage technologies. In lithium-ion batteries, electrolytes with single- or near-single-ion conductivity reduce losses caused by ion polarization. In emergent lithium or sodium metal batteries, they maintain high conductivity at the anode and stabilize metal deposition by fundamental mechanisms. We report that 20- to 300-nm-thick, single-ion-conducting membranes deposited at the anode enable electrolytes with the highest combination of cation transference number, ionic conductivity, and electrochemical stability reported. By means of direct visualization we find that single-ion membranes also reduce dendritic deposition of Li in liquids. Galvanostatic measurements further show that the electrolytes facilitate long (3 mAh) recharge of full Li/LiNi$_{0.8}$Co$_{0.15}$Al$_{0.05}$O$_2$ (NCA) cells with high cathode loadings (3 mAh cm^{-2}/19.9 mg cm^{-2}) and at high current densities (3 mA cm^{-2}).

INTRODUCTION

The high efficiency (>90%) with which chemical energy is reversibly converted to electrical energy in closed electrochemical systems such as batteries is a principal driver of interest in rechargeable lithium battery technology. Although progress has arguably been slow in developing commercial versions of these batteries that significantly outperform—in terms of energy stored per unit mass or volume—the first lithium-ion batteries (LIBs) introduced in the 1990s, significant strides have been made in improving other performance metrics, including cost, efficiency, lifetime, and battery system power density.[1–3] As a result, LIBs are finding applications in a growing list of technologies, including electrified transportation, grid storage, autonomous aircraft (drones), and robotics.[4,5] It is understood that the most productive paths forward in designing batteries that offer the high specific energies and power required by these new applications will include development of electrolytes compatible with higher-voltage intercalating cathodes. Stable anodes that store more charge per unit mass or volume than the currently used LiC_6 material provide a second pathway. Cathodes based on conversion chemistries (e.g., S_8, O_2, CO_2/O_2) also offer potentially large gains in storage capacity. A persistent, fundamental challenge is preserving the high efficiency characteristic of LIB technology in any of these new battery designs.

Efficient electrochemical energy storage in batteries requires facile transport of ions in bulk, typically liquid electrolytes and careful management of reactivity and ion

Context & Scale

Less than three decades after its introduction, lithium-ion battery (LIB) technology dominates the market for portable electrical energy storage (EES) systems for consumer electronics and electric vehicles. Demand for more compact, lighter, more powerful EES solutions to meet needs for advanced electric vehicles and emergent autonomous robotics require more energy-dense lithium-metal batteries (LMBs) that utilize metallic Li anodes. We report on nanometer-thick artificial solid-electrolyte interphases (SEIs) composed of single-ion-conducting ionic polymers tethered to Li electrodes. The SEIs take advantage of synergistic processes for achieving high ionic conductivity, negligible ion polarization, and stable Li deposition. They also protect Li from parasitic reactions with liquid electrolytes, as well as from oxidative degradation on contact with ambient air, simultaneously improving cycling efficiency of LMBs and enabling LMB production using standard, dry-room-based, manufacturing.

transport at explicit interfaces between electrodes and electrolytes. During normal operation, uncontrolled chemical and/or electrochemical reactions of electrolyte components near electrolyte/electrode interfaces produce 10- to 50-nm-thick, ion-conducting membranes composed of organic/inorganic lithium compounds, loosely termed the solid-electrolyte interphase (SEI).[6] Under favorable circumstances the SEI passivates the electrode without compromising interfacial ion transport. In LIBs, for example, typical liquid electrolytes including carbonates, esters, ethers, etc., with dopant salts such as $LiPF_6$ or LiTFSI, have LUMO levels lower than that of a conventional lithiated graphite anode, which in principle should lead to continuous reductive decomposition of the electrolyte.[7,8] The fact that these reactions result in minimal loss of efficiency in today's state-of-the-art LIBs is believed to be a consequence of transport barriers provided by a well-formed and mechanically stable SEI.

Here we report on artificial SEIs created using well-formed and mechanically robust ionomers anchored to the surface of a lithium-metal anode and investigate their structure-property-performance characteristics as a function of membrane thickness in the range from 10 μm to 20 nm. Significantly, we find that single-ion transport properties of even a few-nanometer-thick SEI may be imparted to an entire bulk liquid electrolyte that wets the interfacial material without compromising overall ionic conductivity. On this basis we show that by means of SEI design alone it is possible to achieve liquid electrolytes with high room temperature ionic conductivities and extremely low ion polarization. To our knowledge, this is the first direct demonstration of the critical role a well-formed SEI may play in regulating overall ion and mass transport in batteries. By means of direct visualization and electrochemical analysis, we further show that nanometer-thick artificial SEI are able to selectively transport cations to the Li-metal electrode and lead to large improvements in the metal's ability to deposit smoothly during battery recharge. Finally, it is shown that the single-ion-conducting artificial SEI can be easily integrated with other, previously reported electrolyte design concepts[9,10] to create synergistic methods to suppress metal dendrite proliferation in liquid electrolytes.

The thickness, chemical composition, transport properties, and mechanical features of the SEI are important determinants of long-term battery stability, but little is known fundamentally about structure-property-performance features of these membranes. A well-established and successful practice in the field has been to introduce sacrificial electrolyte additives, such as vinylene carbonate (VC) and more recently fluoroethylene carbonate (FEC), able to preferentially break down and undergo polymerization and ion-exchange reactions at the anode/electrolyte interface to produce SEIs with desirable chemical composition and physical properties.[8] In emergent battery chemistries based on unhosted reactive metal anodes (such as Li and Na), a stable SEI able to accommodate the cyclic volume changes at the anode during charge (addition) and discharge (removal) of metal atoms to the electrode is known to be a requirement for stable long-term cell operation, but relatively little is known about the design rules for such interphases.[11]

In a typical liquid electrolyte, disassociated lithium salts in aprotic solvents generate mobile cations and anions. Consequently, the fraction of the ionic conductivity that stems from motion of the electrochemically active ion (Li^+) or lithium transference number t_{Li+} is typically small. It means that one-half or more of the work done in driving ion motion in the cell is wasted work. Unstable mobile anions may also migrate to regions of high potential gradient and breakdown prior to the solvent and other electrolyte components, contributing to an inhomogeneous SEI and increased interfacial

[1]Department of Materials Science and Engineering, Cornell University, Ithaca, NY 14853, USA

[2]Robert Frederick Smith School of Chemical and Biomolecular Engineering, Cornell University, Ithaca, NY 14853, USA

[3]School of Applied and Engineering Physics, Cornell University, Ithaca, NY 14853, USA

[4]Kavli Institute at Cornell for Nanoscale Science, Cornell University, Ithaca, NY 14853, USA

[5]These authors contributed equally

[6]Lead Contact

*Correspondence: laa25@cornell.edu

http://dx.doi.org/10.1016/j.joule.2017.06.002

resistance. At current densities above the limiting current, theory predicts that an anion depletion zone (or space charge) can be created in an energy battery near the electrode surface, which produces large increases in cell resistance.

Consequences for electrolyte polarization are more severe in emergent battery chemistries such as Li-S, Na-S, Li-O_2/CO_2, Na-O_2/CO_2, and Zn-O_2, which use unhosted metals (e.g., Li, Na, Zn),[12–16] at the anode for 5- to 10-fold improvements in anode storage capacity. In such cells, the existence of a space charge in the electrolyte has been shown to drive unstable electro-convective flows inside the battery, which in turn drives unstable deposition and dendrite formation of the metal during battery recharge.[17,18] The fact that the benefits of the metal anodes carry over to cells in which the anode is paired with a conventional intercalating cathode to produce rechargeable batteries with 2–3 times higher specific storage on a gravimetric or volumetric basis underscores the pressing need for fundamental solutions. Recently a number of approaches, including using single-ion-conducting electrolyte,[19–21] high-modulus separators/electrolyte,[10,22,23] SEI protective agents,[24–27] and non-carbonaceous hosts for lithium,[28,29] have been proposed to overcome these problems for Li-metal cells. The successes and shortcomings of these approaches are discussed in several comprehensive review articles.[11,30,31]

RESULTS AND DISCUSSION

Our specific approach to SEI design focuses on materials that take advantage of synergies identified by recent results from linear stability analysis of electrodeposition of Li.[30,32] In so-called structured electrolytes in which a fraction of anions are anchored to a rigid support, this analysis reveals that the growth rate of dendritic nucleates is determined by two dimensionless parameters, $P_1 = JFL/\upsilon\sigma t_{Li+}G$ and $P_2 = JFL^2/\upsilon\sigma t_{Li+}S$. Here J is the current density, υ is the molar volume of lithium metal, F is the Faraday constant, and L is the distance between the two electrodes. Because the analysis applies to the earliest stages of dendrite growth, P_1 and P_2 are also functions of the electrolyte and SEI properties, including the ionic conductivity σ, the lithium transference number t_{Li+}, surface tension at the electrode/electrolyte interphase S, and mechanical modulus G of the electrolyte and SEI.

Design and Physical Analysis of Ionomer SEIs on Li

Figure 1A reports the configuration of the lithium-metal anodes used in the study. To create an artificial SEI on Li, a thin conformal layer of a perfluorinated ionomer was formed on the surface by a simple solvent-casting process under an Ar atmosphere (see Supplemental Experimental Procedures). The thickness of the coating layer is easily controlled by repeated application of the casting process or by increasing the concentration of ionomer in the carrier solvent. Removal of the solvent was observed to produce tightly adhered ionomer films on Li that cannot be mechanically peeled off without damaging the Li metal. To study the effect of the ionomer on stabilizing lithium deposition, a visualization cell (Figure 1B) that allows direct visualization of Li deposition processes in an optical microscope outfitted with extra-long working distance objectives was developed for the study. In brief, two tungsten rods are used as the circuit connection to lithium-metal electrodes, which are sealed in a two-stage non-tapered, high-quality optical glass tube. As discussed later, visualization measurements using the device demonstrate that an ionomeric SEI with the proposed design has an obvious stabilizing effect on Li deposition.

The success of the SEI transfer procedure is readily confirmed using cryo-focused ion beam scanning electron microscopy (cryo-FIB-SEM), as shown in Figure 1C.

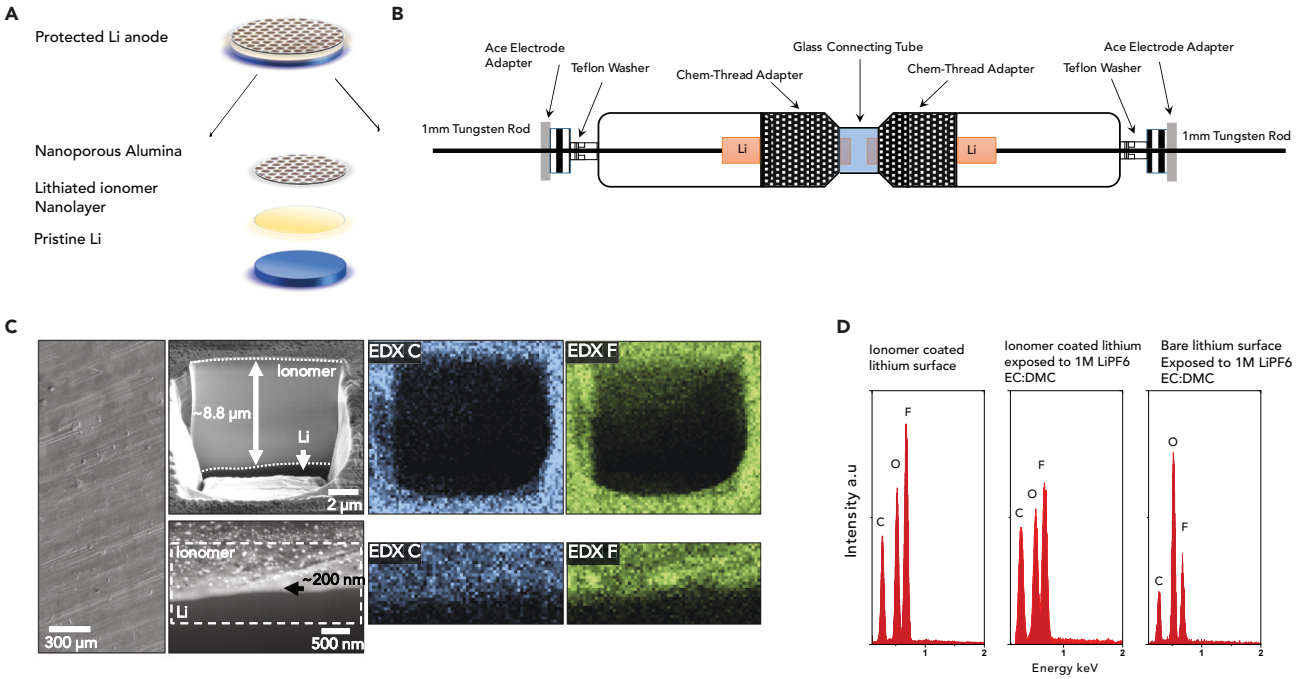

Figure 1. An Ionomer-Based Artificial SEI Protects and Stabilizes the Lithium Anode

(A) Schematic of Lithion-protected Li; see also Scheme S1 and Figure S1.

(B) Customized optical visualization cell for direct observation of lithium electrodeposition at interfaces.

(C) Cryo-FIB-SEM images of ionomer coating on lithium; the first column is an overview image showing the surface morphology of a ~200-nm Lithion coating on Li. The second column shows cross-sections through ~9-µm-thick (top) and ~200-nm-thick (bottom) coatings. The corresponding EDX maps of carbon and fluorine are shown to the right. The scale bar is associated with the length scale in the microscope images.

(D) EDX spectra of Lithion-coated lithium, coated Li exposed to 1 M $LiPF_6$ EC:DMC overnight, and bare Li exposed to 1 M $LiPF_6$ EC:DMC overnight.

Cryogenic temperatures are necessary to ensure well-behaved lithium milling, as lithium reacts with the gallium ions at room temperature. A homogeneous surface coating can be visually examined from the top-view and its thickness and depth-dependent elemental composition determined by imaging and energy-dispersive X-ray (EDX) mapping of cross-sections through the coating produced by FIB milling. Our cryo-FIB measurements show that coatings with tunable thicknesses in the range of sub-100 nm up to nearly 10 µm are achieved. Fourier transform infrared spectra provide additional information about the ionomer coatings, as shown in Figure S1. Compared with pristine lithium, pronounced broad peaks appear at 1,150 cm^{-1} and 1,240 cm^{-1} on ionomer-coated Li, which can be assigned to the symmetric and asymmetric C-F bond stretching, respectively, a signature of the perfluorinated ionomer backbone.[33] These features remain even after the ionomer-coated lithium is exposed to the electrolyte. Figure 1D compares EDX spectra of a lithium substrate before and after overnight exposure to 1 M $LiPF_6$ ethylene carbonate (EC):dimethyl carbonate (DMC) liquid electrolyte. Both spectra exhibit a large fluorine-to-carbon ratio compared with the pristine lithium after contacting the electrolyte. The results mean that the ionomer coating on Li is stable in the electrolyte solvent and shows that an ionomer-based SEI created on Li is compatible with the most commonly used carbonate-based liquid electrolytes.

A general concern regarding the protection of any anode with an artificial SEI is whether the coating material, usually composed of a moderately ionic-conductive polymer or ceramic, could achieve comparable levels of interfacial ion transport in a spontaneously formed thin SEI film. Figure 2 reports on the ion transport

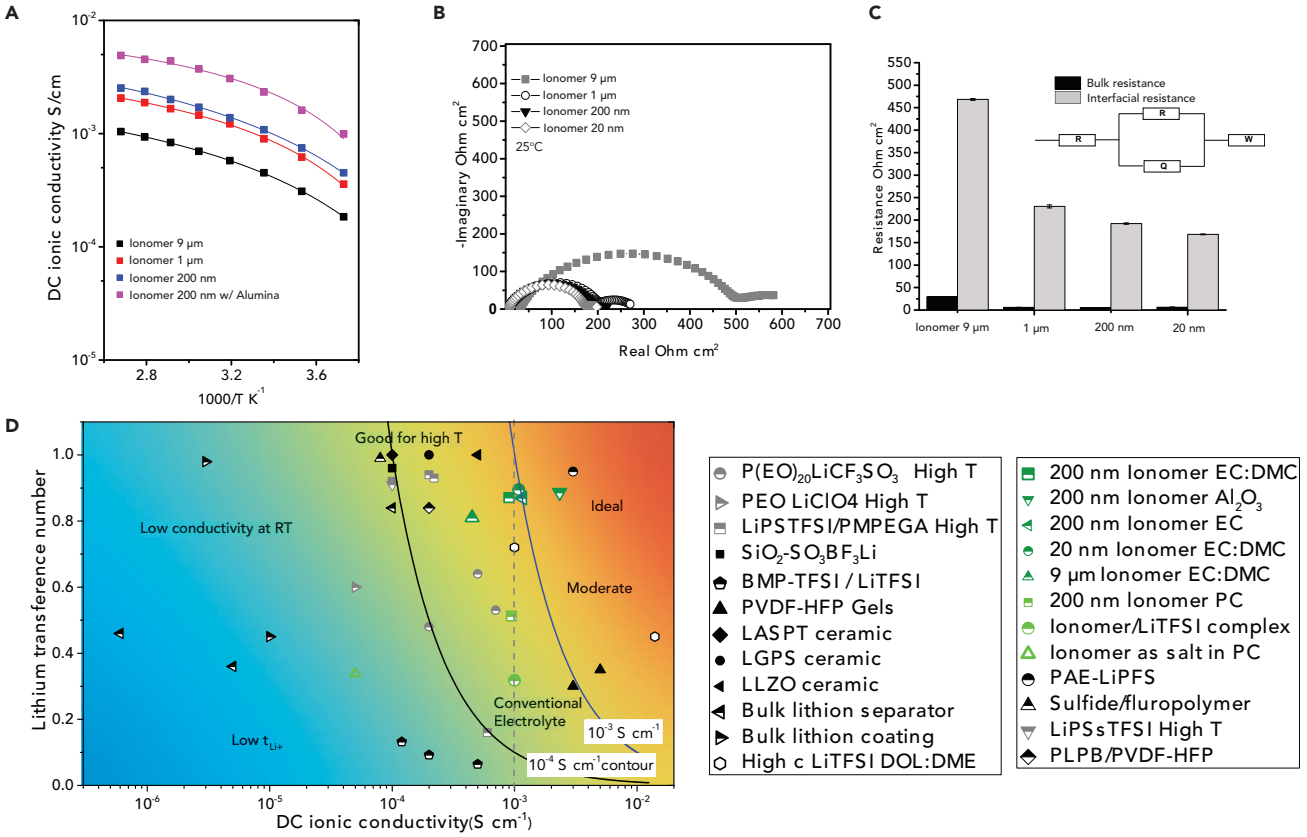

Figure 2. Electrochemical and Physical Properties of Ionomer-Protected Lithium Anodes

(A) Temperature-dependent ionic conductivity as a function of coating thickness.

(B) Electrochemical impedance spectra at 25°C of symmetric cells with Li electrodes protected by Lithion with different thicknesses; see also Tables S1 and S2.

(C) Fitted bulk and interfacial resistance using the equivalent circuit model shown in the inset. The error bars are associated with the circuit fitting.

(D) A summary figure comparing ionic conductivity and lithium transference number of various electrolyte systems, including those reported in the present study (green symbols). Gray symbols represent conductivity values measured above room temperature. Solid and open symbols represent results for solid-state and liquid electrolytes, respectively. Half-filled symbols are results for composite/hybrid electrolytes. Conductivity contour lines are drawn to highlight contributions to the total conductivity that arises from motion of Li ions. Detailed information is included in the supporting information. See also Tables S3 and S4.

properties of the ionomer SEI on Li in the context of a symmetric lithium battery. The temperature-dependent DC ionic conductivity, as shown in Figure 2A, exhibits a liquid-like, high ionic conductivity within the range of normal battery operation temperatures, and is described well by the classic Vogel-Fulcher-Tammann equation for liquid electrolytes. The fact that the overall ionic conductivity of the electrolyte is observed to increase as the ionomer coating thickness is reduced is as expected, but also testifies to the already significant effect the thickness and properties of the SEI have on ion transport in an electrolyte. It is observed further that at coating thickness below 200 nm, the conductivity exceeds 1×10^{-3} S cm^{-1} at room temperature, comparable with that of a typical liquid electrolyte. Even with the thickest coating studied, the room temperature conductivity is still high (approximately 5×10^{-4} S cm^{-1}), indicating that an ionomeric SEI provides a promising design for preserving fast interfacial ion transport while other features of a desirable SEI are manipulated. Significantly, it is also seen that when the coatings are co-deposited with a layer of nanoporous Al_2O_3, shown in earlier work to prohibit dendritic deposition of Li, moderately higher ionic conductivity is observed, simultaneously

confirming the compatibility of the coatings with other electrolyte design concepts and confirming that the coatings do not hinder the high ion mobility within the nanochannels reported in our previous work.[34]

Electrochemical Analysis of Ionomer SEI on Li

More direct knowledge of how an ionomeric SEI influences interfacial ion transport can be deduced from electrochemical impedance spectroscopy. Figures 2B and 2C compare the impedance spectra of ionomer-coated lithium/lithium symmetric cells with a coating thickness ranging from 20 nm to 9 μm. Spectra were fit to the equivalent circuit model shown, allowing the bulk and interfacial resistance per area to be determined (Table S1). Consistent with the results reported in Figure 2A, a moderately high bulk resistance of about 23 ohm cm^{-2} is observed for the thickest coating (9 μm), which is already bulk-like, in comparison with the interelectrode distance (~25 μm). The interfacial resistance, however, is seen to decrease drastically with thickness of the ionomer coating. In particular, it is seen that for thicknesses below 200 nm, the interfacial resistance is about 150 ohm cm^{-2}, close to the value of freshly polished lithium foil. More detailed analysis on impedance spectra involves dissecting interphases individually in the fitting model, as reported in Table S2. The impedance from the ionomer coating mainly arises from the ionomer/liquid interphase and the bulk ionomer resistance, which supports the hypothesis that the ions are selected for transport through the interphase. Additionally the ionomeric coating makes the protected lithium moderately resistant to oxidation in the ambient air environment, evidenced by a slow build-up of interfacial resistance over 3 hr in a cell allowing air flow through the cap and the current collector (see Figure S2). These observations indicate that ions are efficiently transported from the liquid electrolyte to the Li electrode surface.

An even more interesting finding is the effect that an ionomer-based SEI has on more subtle aspects of ion transport and electrolyte polarization. Figure 2D reports the lithium transference number (t_{Li+}) measured in Li cells with/without the ionomer SEI. For comparison, the heatmap compares the measured values of the t_{Li+} achieved with those of other materials reported in the literature, in each case benchmarking the results against the ionic conductivity reported for the same materials. In a typical liquid electrolyte with binary lithium salt, the t_{Li+} usually is between 0.1 and 0.4.[35] It is apparent from the figure that the Li electrodes coated with an ionomer SEI of arbitrary thickness in the range studied delivers among the highest combination of t_{Li+} and ionic conductivity of materials reported thus far. More fundamentally interesting is the fact that without the ionomer coating, t_{Li+} values for the electrolyte used for the measurements, EC:DMC with 1 M $LiPF_6$ salt, are low (~0.3), in agreement with literature reports.[36] It is also apparent that electrolytes fall into several regions as identified by the colors in the figure. Ionic conductivity >5 × 10^{-4} S cm^{-1} are typically required for stable room temperature battery operation. Conventional liquid electrolytes meet this requirement, but have low t_{Li+}. As indicated by the materials that fall in the yellow regions, successful efforts aimed at improving the t_{Li+} for such electrolytes have been reported based on composite salt and polymer/ceramic frameworks. However, these materials are typically limited by their low room temperature ionic conductivity. Consequently, the fraction of the ion transport contributed by mobile cations is still compromised. The figure also shows contour lines of lithium-ion conductivity of 10^{-4} and 10^{-3} S cm^{-1}, between which most materials targeted for practical battery application must fall.

Higher t_{Li+} can be achieved in lithium-ion-conducting polymer, ceramics, or other types of composites with immobilized anion species (Table S3). However, these

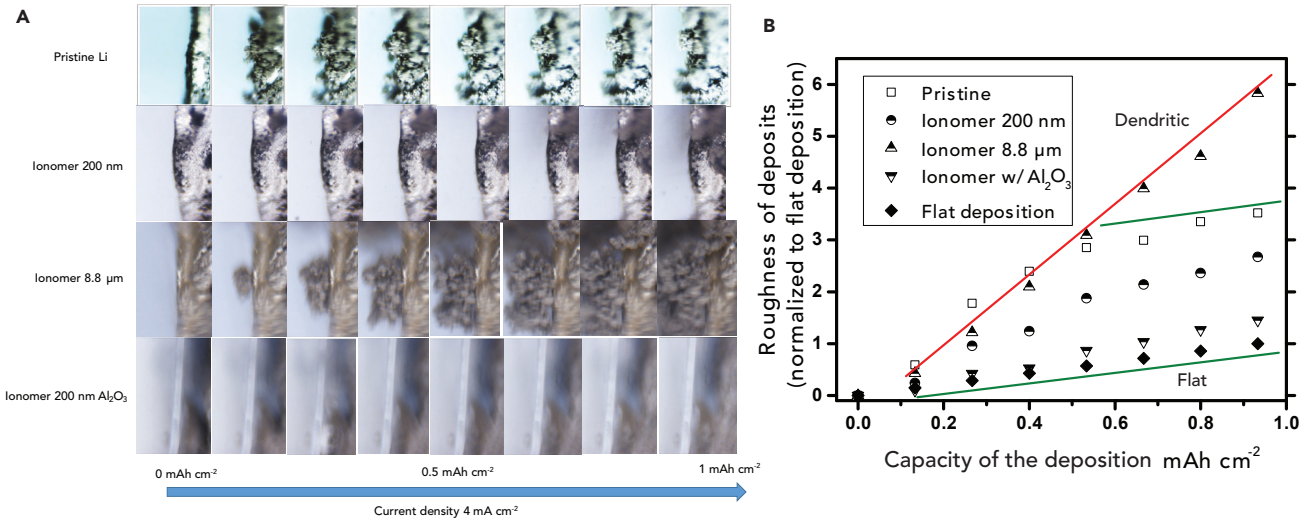

Figure 3. Visualization of Lithium-Metal Electrodeposition in Various Electrolytes

(A) Snapshots of the lithium deposition in a custom-made optical visualization cell that uses pristine lithium, 200-nm-thick ionomer-coated lithium, 9-μm-thick ionomer-coated lithium, and 200-nm-thick ionomer-coated lithium with nanoporous Al_2O_3 (from top to bottom), during the deposition of 1 mAh cm^{-2} of lithium at a current density of 4 mA cm^{-2}.

(B) Normalized dimensionless roughness of deposits as a function of charge passed for the systems in (A). The green line through the data demarcates the base state for "flat" deposition and the red line indicates rough, dendritic deposition.

materials also exhibit moderate or low ambient temperature ionic conductivity and as such are only of practical interest in applications where elevated temperature battery operation is permissible. We have also previously reported on transport properties of bulk perfluorinated lithium conducting ionomer membranes and have shown that these materials offer near-single-ion transport and exceptional ability to stabilize Li-metal deposition,[19,37] yet because of their low ionic conductivity of $<10^{-4}$ S cm^{-1}, the cells are limited to operating at impractically low current density. In contrast, by incorporating a few-nanometers-thick (e.g., 20 nm) ionomer SEI on the electrode the overall t_{Li+} for the cell rises to 0.88 and the room ionic conductivity remains high, approximately 1×10^{-3} S cm^{-1} at room temperature. It is also noted that the ionomer SEI/PC solution does not result in a high t_{Li+}, likely due to the ability of PC (the ionomer solvent used in the solvent-casting step) to dissolve the SEI[19] to produce some unknown fraction of mobile polymer chains in the solvent. This result strengthens the understanding that the immobilized ionomer coating on the lithium/electrolyte interphase does in fact play the dominant role in altering the lithium-ion transport behavior. The unusual high ionic conductivity and high lithium transference number imparted by the ionomer SEI is also significant because it defines a straightforward path for breaking the conventional trade-off[38] between these two important properties in any battery.

Stability of Li Electrodeposition on Ionomer-Coated Electrodes

To further evaluate the effect of the high t_{Li+} values achieved by means of our ionomer SEI, we investigated the stability of lithium-metal deposition on substrates protected by the SEI. Unlike previous studies, where stability was evaluated indirectly from voltage and current measurements during battery cycling, here we employed a customized optical visualization cell (Figure 1B) that can be mounted on the sampling platform of any optical microscope to monitor the metal interface in real time. Here we first consider changes in the interface structure under unidirectional polarization at constant current density in a symmetric lithium cell constructed from two cylindrical lithium electrodes. Figure 3A shows snapshots of the electrodeposition

process under a current density of 4 mA cm^{-2}, which is above the diffusion-limiting current, $J_{OL} = 2zcFD/[L(1 - t_{Li+})] \approx 2.5$ mA cm^{-2}, comprising ions with valency z, concentration c, and binary diffusivity D; L being the interelectrode distance. It is obvious from the images that the deposition on bare lithium electrode quickly becomes unstable and at a capacity as low as 0.1 mAh cm^{-2} the proliferation of mushroom-like, dendritic structures across the electrode surface occurs. In contrast, electrodes with a 200-nm-thick ionomer SEI are seen to suppress uncontrollable and rough electrodeposition, with compact, smooth electrode surfaces observed at more than ten times the deposition capacity at which unprotected Li is unstable. A common perspective in the field is that unstable deposition of reactive metals such as Li and Na at moderate current densities is a consequence of the unstable and heterogeneous SEI formed naturally on these metals by spontaneous reaction with electrolyte components.[13] We are able to directly evaluate this hypothesis by depositing thick (>1 μm) conformal coatings of the ionomer on Li. Our experiments clearly show that in the case of a very thick ionomer SEI (9 μm) an Li electrode is as unstable to dendritic deposition as the unmodified Li electrode. It is noted, however, that unlike the pristine Li electrode, the dendrites appear at a few local sites on the electrode, rather than distributed densely over the surface. One possible explanation of this observation is that a thick ionomer coating renders an overall high interfacial resistance so that ions deposit preferentially on defects in the coatings (e.g., at areas where the ionomer coating thickness is low or where poor coverage or pinholes may exist). Our results therefore indicate that an optimal ionomer SEI thickness is essential for achieving uniform electrodeposits at moderate to high current density. We also evaluated the combined effect of an ionomer SEI and nanoporous Al_2O_3 membranes reported in our previous work[34] to also stabilize Li deposition. It is seen that smooth deposition is achieved and there is no sign of dendrite penetration through the Al_2O_3 membrane.

Figure 3B quantifies the effects observed in Figure 3A in terms of an effective roughness factor. The roughness here is characterized as the ratio between the deposition area deduced using ImageJ image analysis software and the surface area of a theoretical flat deposit. It is apparent that the surface roughness evolves in two regimes, identified by the green line (flat deposition) and the red line (dendritic growth). In accordance with the visual inspection, the 200-nm-thick ionomer-protected symmetric cell with nanoporous Al_2O_3 membranes shows the least roughness, which is close to the trend of flat deposition, underscoring the need to have a strong separator/electrolyte in the lithium cells. Even without the Al_2O_3 membrane, the ionomer coating with 200 nm thickness still retards the proliferation of rough deposits by nearly two times compared with the bare lithium. In both cases, the increase of roughness slows down after depositing 0.3 mAh cm^{-2} of lithium. This may be due to the orphaned lithium ceasing to grow, meaning that the deposition would happen at other locations not captured by the microscope scanning region. However, it is surprising to observe that with a 9-μm-thick ionomer coating a nearly linear increase of roughness with time is observed, following the red line. This is likely due to the continuous growth of dendrite stems beneath the thick coating, which supports our hypothesis that sparse electrodeposits formed at a few sparse sites as a consequence of conductivity limitation from the thick coating.

Typically, the diffusion-limiting current in a battery is orders of magnitude higher than what can be achieved in our visualization cell, due to larger interelectrode distance in the latter. To understand the effect of an ionomer SEI on battery operation at practical current densities, we performed postmortem scanning electron microscopic analysis of electrodes harvested from coin cells. As shown in Figure S3, results

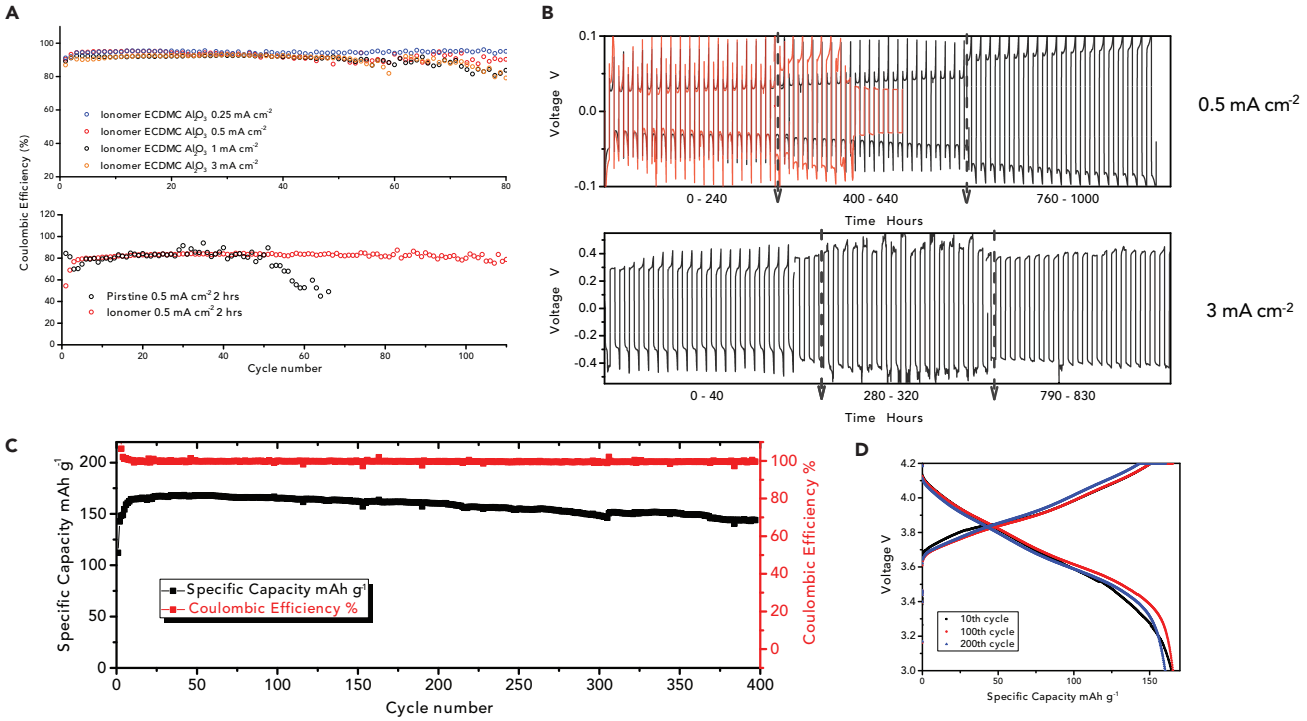

Figure 4. Cycling Performance of Rechargeable LMBs Based on Lithion-Protected Li Anodes

(A) Coulombic efficiency (CE) as a function of cycle number for 200-nm-thick ionomer-protected and nanoporous Al_2O_3-protected Li/Cu electrodes at current densities of 0.25, 0.5, and 1 mA cm^{-2} for 1 mAh cm^{-2} per plating/stripping, and 3 mA cm^{-2} for 3 mAh cm^{-2} per plating/striping. In all cases an electrolyte blend composed of 1 M $LiPF_6$ EC:DMC + 10% FEC + 1% VC was employed for the studies. The bottom figure compares the CE for 200-nm-thick ionomer-protected Li with unprotected Li electrodes in the baseline electrolyte containing no FEC or VC additives.

(B) Lithium plating/striping voltage profile for the ionomer and nanoporous Al_2O_3-protected lithium at 0.5 and 3 mA cm^{-2} for 3 mAh cm^{-2} per plating/stripping. Here the red line corresponds to bare lithium.

(C) Full cells comprising 200-nm-thick ionomer-protected and nanoporous Al_2O_3-protected Li versus NCA cathode with 3 mAh cm^{-2} areal capacity operated at 0.5 C.

(D) Voltage-specific capacity profile for a 200-nm-thick ionomer- and nanoporous Al_2O_3-protected Li/NCA cell.

from these experiments support the conclusions from the *in situ* observation. It is seen, for instance, that a 200-nm-thick ionomer coating on Li yields a compact, uniform Li deposit morphology even after 3 mAh cm^{-2} of charge. In contrast, electrodes harvested from cells composed of unmodified Li exhibit obviously rougher, mossy dendrites. Consistent with the results from visualization experiments, thicker ionomer SEIs again exhibit larger, rougher electrodeposits sparsely distributed on the electrode surface. Postmortem FIB-SEM observation (Figure S5) shows that there are no large lithium deposits above the ionomer layer where FIB cross-sections were taken. FIB-SEM analysis of the electrodes in cells cycled to varying extents (1–100 cycles) indicate that while there is variation of the ionomer thickness during cycling, the ionomer coatings generally appear to become slightly thicker with cycling. We have tentatively attributed this observation to swelling of the coating as a result of extended exposure to the electrolyte solvent and/or physical deformation induced by repeated lithium plating/stripping cycles.

Figure 4 reports galvanostatic cycling experiments in cells that utilize a 200-nm-thick ionomer SEI and a nanoporous Al_2O_3 membrane with 20 nm pore diameter. Figure 4A compares the Coulombic efficiency (CE) of this lithium/ionomer/Al_2O_3/Cu cell with a pristine lithium/Cu cell during a lithium plating/stripping experiment with conventional EC:DMC liquid electrolyte. It is seen that the ionomer has a

protective effect on the Li anode against parasitic side reactions with the electrolyte, leading to moderately high (>92%) and stable CEs in extended cycling. Similar improvements are apparent at a current density of 3 mA cm^{-2} from 3 mAh cm^{-2} plate/strip cycling experiments. The bottom plot in Figure 4A in fact indicates that an ionomer SEI on Li exhibits moderately high and stable CE profiles. This can be contrasted with cells based on unmodified Li electrodes that show an initial CE of ~86% that deteriorates quickly within 30 cycles, after which the lithium plating/stripping becomes unstable. We note, however, that while a CE of 92% is an improvement over the pristine Li case, the increase is not large enough to produce stable cycling of a practical Li cell in which the Li excess is ideally zero. The less than ideal CE values for the ionomer-coated Li electrodes are thought to originate from two sources, both related to the inherent chemical instability of DMC upon long-term exposure to metallic Li. First, the counter electrode in the CE experiments is an uncoated copper foil, which means that for at least half of the duration of an Li plate/strip cycle, freshly deposited Li at the Cu electrode is unprotected and in direct contact with the liquid electrolyte. Second, the ionomer preserves high, liquid-like overall transport of Li ions by absorbing sufficient liquid electrolyte to facilitate fast interfacial transport of Li. This means that freshly deposited Li even at the "protected" Li electrode will also be in direct contact with some volume of liquid electrolyte. The resultant degradation of the electrolyte at both electrodes may be expected over time to change the chemical composition and transport properties of the interphases, which is in fact consistent with our observations (see Table S4). Our findings mean that in order to simultaneously achieve high transference numbers, stable Li deposition, and high CE values, the ionomer coatings must be used in tandem with a liquid electrolyte with intrinsic chemical stability upon extended contact with metallic Li. Results reported in Figure S4 show that this expectation is indeed met using pure EC as the electrolyte solvent. The figure shows that even without efforts to optimize the electrolyte composition or to protect the Cu counter electrode, CE values as high as 98% can be achieved for ionomer-coated Li electrodes cycled in this electrolyte. The results underscore the complementary need for stable artificial interphases and stable electrolytes for enabling LMBs.

The long-term lithium plating/stripping performance in the baseline EC:DMC electrolyte was evaluated in lithium/lithium symmetric cells (Figure 4B), with both electrodes protected by ionomer coating. At a moderate current density of 0.5 mA cm^{-2} and 6 hr per charge/discharge step, the lifetime is at least doubled relative to cells based on unmodified Li electrodes, which are seen to exhibit a sudden drop in voltage (red line) after a small number of cycles. Similar results are seen when cells are cycled at a higher, more practical current density of 3 mA cm^{-2} for 1 hr per charge/discharge. It is noted that in this case, even after 800 hr of continuous testing, the voltage profile displays no signs of failure by dendrite-induced short circuits. It is noted, nonetheless, that at intermediate cycles, occasional voltage spikes are observed during cycling at the higher rates. We tentatively attribute these spikes to side reactions associated with the ionomer SEI.

Analysis in Half-Cell → Full-Cell LMBs Based on Intercalating Cathodes

As a final assessment of the ionomer SEI, we investigated galvanostatic cycling of what we loosely term a "half-cell → full cell," whereby a conventional intercalating $LiNi_{0.8}Co_{0.15}Al_{0.05}O_2$ (NCA) cathode with high active material mass loading (3 mA cm^{-2} or 19.9 mg cm^{-2}) is paired with a metallic lithium anode. Figures 4C and 4D report the specific capacity and CE of these Li-NCA cells operated at 0.5 C. It is seen that within 400 cycles of charge and discharge there is at most a 6% loss of capacity, and the CE remains close to unity. The voltage profiles show there is minimal

over-potential increase during extended cycling, which is attributed to the stable interfacial resistance that the ionomer SEI provides the Li electrode. Figure S6 reports results from postmortem analysis of an ionomer/Al_2O_3-protected lithium surface after extensive full-cell cycling. A uniform lithium surface is observed and there is no sign of clogging of the Al_2O_3. EDX analysis reveals a strong fluorine signal from primary fluorinated compounds, which is confirmed by X-ray photoelectron spectroscopy analysis (Figure S7). This indicates that in addition to the stabilizing effect of the single- or near-single-ion transport enabled by the ionomer SEI, spontaneous formation of species such as LiF at the anode may play a role in the exceptional stability that the ionomer SEI imparts to Li.[25,26,39] Figure S8 reports results from floating experiments using protected/unprotected Li as anode and NCA as cathode. Voltages in the range 3.8–5 V were used for the experiments with each voltage step lasting for 24 hr. Cells based on the ionomer-protected Li are seen to exhibit much lower leakage currents above 4.1 V compared with those based on pristine Li anodes. This observation is consistent with the existence of a stable SEI that stabilizes the electrolyte against electrochemical decomposition at potentials beyond its stability limit. Even smaller leakage currents are seen after initial battery cycling, whereby for floating voltages up to 5 V a leakage current <10 $\mu A\ cm^{-2}$ is measured. To further evaluate the stability of the interphase, fresh electrolyte (>100 μL) was added to some of the pre-cycled cells and the floating voltage reinstated. The leak current remains quite low, indicating that the ionomer interphase remains robust and strong.

EXPERIMENTAL PROCEDURES

Full details of all experiments are provided in Supplemental Experimental Procedures.

Summary

We have demonstrated that artificial SEI based on nanometer-thick ionomer coatings on Li-metal electrodes stabilize the electrodes in long-term cycling studies performed in both over-limiting current and diffusion-allowed regimes. The SEIs appear to protect Li from direct contact with liquid electrolyte, but do not compromise interfacial mobility of Li+ at the electrolyte/Li interface. Significantly, we also find that ionomer coating on Li of even a few nanometers thick fundamentally alters ion transport behavior in the entire cell, achieving a high lithium transference number close to 0.9 even in generic carbonate-based electrolytes doped with standard salts. Direct visualization studies show that an ionomer SEI on Li leads to a flatter, more uniform deposition of the metal, but that the effect disappears when the SEI thickness becomes too large. When integrated in lithium-metal batteries (LMBs) that employ nanoporous membranes as separators, and either copper, metallic lithium, or an NCA as the counter electrode, we find that the protected Li anodes exhibit long-term failure-free lithium plating/striping in a carbonate-based electrolyte at high current density of 3 $mA\ cm^{-2}$ for over 800 hr for 3 $mAh\ cm^{-2}$ capacity per cycle. Similar highly stable and efficient full-cell operation with less than 11% capacity fade over 400 cycles is also reported in Li/NCA cells, in which the active material loading in the cathode is high (3 $mAh\ cm^{-2}$). Our results provide a path toward SEI design that enables high energy and safe LMBs. They also provide a path for achieving higher efficiency charge transport in rechargeable batteries of all types through regulated ion transport in artificial SEIs tethered to the electrodes.

SUPPLEMENTAL INFORMATION

Supplemental Information includes Supplemental Experimental Procedures, nine figures, four tables, and one scheme and can be found with this article online at http://dx.doi.org/10.1016/j.joule.2017.06.002.

AUTHOR CONTRIBUTIONS

Conceptualization, Z.T., S.C., and L.A.A.; Methodology, Z.T., S.C., M.J.Z., L.F.K., and L.A.A.; Investigation, Z.T., S.C., M.J.Z., S.W., and K.Z.; Writing – Original Draft, Z.T. and L.A.A; Writing – Review & Editing, Z.T., S.C., M.J.Z., L.F.K., and L.A.A.; Funding Acquisition, L.F.K. and L.A.A.; Resources, L.F.K. and L.A.A.; Supervision, L.F.K. and L.A.A.

ACKNOWLEDGMENTS

This work was supported by the Department of Energy, Advanced Research Projects Agency – Energy (ARPA-E) through award #DE-AR0000750. M.J.Z. and L.F.K. acknowledge support by the NSF (DMR-1654596). The work made use of electrochemical characterization facilities in the KAUST-CU Center for Energy and Sustainability, supported by the King Abdullah University of Science and Technology (KAUST) through award #KUS-C1-018-02. Electron microscopy facilities at the Cornell Center for Materials Research (CCMR), an NSF-supported MRSEC through grant DMR-1120296, were also used for the study. Additional support for the FIB/SEM cryo-stage and transfer system was provided by the Kavli Institute at Cornell and the Energy Materials Center at Cornell, DOE EFRC BES (DE-SC0001086). Z.T. thanks Bryant Polzin for kindly providing NCA cathode materials from the Cell Analysis, Modeling, and Prototyping (CAMP) Facility at Argonne National Laboratories.

Received: April 1, 2017
Revised: May 20, 2017
Accepted: June 20, 2017
Published: September 20, 2017

REFERENCES

1. Tarascon, J.M., and Armand, M. (2001). Issues and challenges facing rechargeable lithium batteries. Nature *414*, 359–367.
2. Armand, M., and Tarascon, J.M. (2008). Building better batteries. Nature *451*, 652–657.
3. Yoshino, A. (2012). The birth of the lithium-ion battery. Angew. Chem. Int. Ed. *51*, 5798–5800.
4. Etacheri, V., Marom, R., Elazari, R., Salitra, G., and Aurbach, D. (2011). Challenges in the development of advanced Li-ion batteries: a review. Energy Environ. Sci. *4*, 3243–3262.
5. Dunn, B., Kamath, H., and Tarascon, J.-M. (2011). Electrical energy storage for the grid: a battery of choices. Science *334*, 928–935.
6. Xu, K. (2014). Electrolytes and interphases in Li-ion batteries and beyond. Chem. Rev. *114*, 11503–11618.
7. Aurbach, D., Talyosef, Y., Markovsky, B., Markevich, E., Zinigrad, E., Asraf, L., Gnanaraj, J.S., and Kim, H.-J. (2004). Design of electrolyte solutions for Li and Li-ion batteries: a review. Electrochim. Acta *50*, 247–254.
8. Goodenough, J.B., and Kim, Y. (2009). Challenges for rechargeable Li batteries. Chem. Mater. *22*, 587–603.
9. Tu, Z., Lu, Y., and Archer, L. (2015). A dendrite-free lithium metal battery model based on nanoporous polymer/ceramic composite electrolytes and high-energy electrodes. Small *11*, 2631–2635.
10. Tu, Z., Kambe, Y., Lu, Y., and Archer, L.A. (2014). Nanoporous polymer-ceramic composite electrolytes for lithium metal batteries. Adv. Energy Mater. *4*, http://dx.doi.org/10.1002/aenm.201300654.
11. Cheng, X.B., Zhang, R., Zhao, C.Z., Wei, F., Zhang, J.G., and Zhang, Q. (2015). A review of solid electrolyte interphases on lithium metal anode. Adv. Sci. *3*, http://dx.doi.org/10.1002/advs.201500213.
12. Tu, Z., Nath, P., Lu, Y., Tikekar, M.D., and Archer, L.A. (2015). Nanostructured electrolytes for stable lithium electrodeposition in secondary batteries. Acc. Chem. Res. *48*, 2947–2956.
13. Lin, D., Liu, Y., and Cui, Y. (2017). Reviving the lithium metal anode for high-energy batteries. Nat. Nanotechnol. *12*, 194–206.
14. Aurbach, D., McCloskey, B.D., Nazar, L.F., and Bruce, P.G. (2016). Advances in understanding mechanisms underpinning lithium-air batteries. Nat. Energy *1*, 16128.
15. Pang, Q., Liang, X., Kwok, C.Y., and Nazar, L.F. (2016). Advances in lithium-sulfur batteries based on multifunctional cathodes and electrolytes. Nat. Energy *1*, 16132.
16. Li, Y., and Dai, H. (2014). Recent advances in zinc-air batteries. Chem. Soc. Rev. *43*, 5257–5275.
17. Chazalviel, J.N. (1990). Electrochemical aspects of the generation of ramified metallic electrodeposits. Phys. Rev. A *42*, 7355–7367.
18. Rosso, M., Gobron, T., Brissot, C., Chazalviel, J.-N., and Lascaud, S. (2001). Onset of dendritic growth in lithium/polymer cells. J. Power Sources *97*, 804–806.
19. Lu, Y., Tikekar, M., Mohanty, R., Hendrickson, K., Ma, L., and Archer, L.A. (2015). Stable cycling of lithium metal batteries using high transference number electrolytes. Adv. Energy Mater. *5*, http://dx.doi.org/10.1002/aenm.201402073.
20. Bouchet, R., Maria, S., Meziane, R., Aboulaich, A., Lienafa, L., Bonnet, J.-P., Phan, T.N., Bertin, D., Gigmes, D., and Devaux, D. (2013). Single-ion BAB triblock copolymers as highly efficient electrolytes for lithium-metal batteries. Nat. Mater. *12*, 452–457.
21. Srivastava, S., Schaefer, J.L., Yang, Z., Tu, Z., and Archer, L.A. (2014). 25th anniversary article: polymer-particle composites: phase stability and applications in electrochemical energy storage. Adv. Mater. *26*, 201–234.
22. Khurana, R., Schaefer, J.L., Archer, L.A., and Coates, G.W. (2014). Suppression of lithium dendrite growth using cross-linked polyethylene/poly (ethylene oxide) electrolytes: a new approach for practical lithium-metal polymer batteries. J. Am. Chem. Soc. *136*, 7395–7402.
23. Tung, S.-O., Ho, S., Yang, M., Zhang, R., and Kotov, N.A. (2015). A dendrite-suppressing composite ion conductor from aramid nanofibres. Nat. Commun. *6*, http://dx.doi.org/10.1038/ncomms7152.

24. Ding, F., Xu, W., Graff, G.L., Zhang, J., Sushko, M.L., Chen, X.L., Shao, Y.Y., Engelhard, M.H., Nie, Z.M., Xiao, J., et al. (2013). dendrite-free lithium deposition via self-healing electrostatic shield mechanism. J. Am. Chem. Soc. *135*, 4450–4456.

25. Lu, Y., Tu, Z., and Archer, L.A. (2014). Stable lithium electrodeposition in liquid and nanoporous solid electrolytes. Nat. Mater. *13*, 961–969.

26. Zhang, X.Q., Cheng, X.B., Chen, X., Yan, C., and Zhang, Q. (2017). Fluoroethylene carbonate additives to render uniform li deposits in lithium metal batteries. Adv. Funct. Mater. *27*, http://dx.doi.org/10.1002/adfm.201605989.

27. Li, W., Yao, H., Yan, K., Zheng, G., Liang, Z., Chiang, Y.-M., and Cui, Y. (2015). The synergetic effect of lithium polysulfide and lithium nitrate to prevent lithium dendrite growth. Nat. Commun. *6*, http://dx.doi.org/10.1038/ncomms8436.

28. Lin, D., Liu, Y., Liang, Z., Lee, H.-W., Sun, J., Wang, H., Yan, K., Xie, J., and Cui, Y. (2016). Layered reduced graphene oxide with nanoscale interlayer gaps as a stable host for lithium metal anodes. Nat. Nanotechnol. *11*, 626–632.

29. Liang, Z., Lin, D., Zhao, J., Lu, Z., Liu, Y., Liu, C., Lu, Y., Wang, H., Yan, K., and Tao, X. (2016). Composite lithium metal anode by melt infusion of lithium into a 3D conducting scaffold with lithiophilic coating. Proc. Natl. Acad. Sci. USA *113*, 2862–2867.

30. Tikekar, M.D., Choudhury, S., Tu, Z., and Archer, L.A. (2016). Design principles for electrolytes and interfaces for stable lithium-metal batteries. Nat. Energy *1*, 16114.

31. Xu, W., Wang, J.L., Ding, F., Chen, X.L., Nasybutin, E., Zhang, Y.H., and Zhang, J.G. (2014). Lithium metal anodes for rechargeable batteries. Energy Environ. Sci. *7*, 513–537.

32. Tikekar, M.D., Archer, L.A., and Koch, D.L. (2016). Stabilizing electrodeposition in elastic solid electrolytes containing immobilized anions. Sci. Adv. *2*, e1600320.

33. Liang, Z., Chen, W., Liu, J., Wang, S., Zhou, Z., Li, W., Sun, G., and Xin, Q. (2004). FT-IR study of the microstructure of Nafion® membrane. J. Membr. Sci. *233*, 39–44.

34. Tu, Z., Zachman, M.J., Choudhury, S., Wei, S., Ma, L., Yang, Y., Kourkoutis, L.F., and Archer, L.A. (2017). Nanoporous hybrid electrolytes for high-energy batteries based on reactive metal anodes. Adv. Energy Mater. 1602367, http://dx.doi.org/10.1002/aenm.201602367.

35. Zhao, J., Wang, L., He, X., Wan, C., and Jiang, C. (2008). Determination of lithium-ion transference numbers in LiPF6-PC solutions based on electrochemical polarization and NMR measurements. J. Electrochem. Soc. *155*, A292–A296.

36. Zugmann, S., Fleischmann, M., Amereller, M., Gschwind, R.M., Wiemhöfer, H., and Gores, H. (2011). Measurement of transference numbers for lithium ion electrolytes via four different methods, a comparative study. Electrochim. Acta *56*, 3926–3933.

37. Cai, Z., Liu, Y., Liu, S., Li, L., and Zhang, Y. (2012). High performance of lithium-ion polymer battery based on non-aqueous lithiated perfluorinated sulfonic ion-exchange membranes. Energy Environ. Sci. *5*, 5690–5693.

38. Fergus, J.W. (2010). Ceramic and polymeric solid electrolytes for lithium-ion batteries. J. Power Sources *195*, 4554–4569.

39. Lu, Y., Tu, Z., Shu, J., and Archer, L.A. (2015). Stable lithium electrodeposition in salt-reinforced electrolytes. J. Power Sources *279*, 413–418.